Measuring Wide Angle Antenna Performance Using Small Cylindrical Scanners

S.F. Gregson[#1], C.G. Parini[*2], J. Dupuy[*3]

[#]*Nearfield Systems Inc.*
19730 Magellan Drive, Torrance, CA 90502, USA
[1]sgregson@nearfield.com

[*]*Queen Many, University of London*
School of Electronic Engineering & Computer Science
Mile End Road, London, E1 4NS, UK
[2]c.g.parini@elec.qmul.ac.uk
[3]j.dupuy@elec.qmul.ac.uk

***Abstract*— A near-field measurement technique for the prediction of wide-angle asymptotic far-field antenna patterns from data obtained from a modified small combination planar/cylindrical near-field measurement system is presented. This novel technique utilises a simple change in the alignment of the robotic positioners to enable near-field data to be taken over the surface of a conceptual right conic frustum. This configuration allows existing facilities to characterise wide-angle antenna performance in situations where hitherto they could have been limited by the effects of truncation. This paper aims to introduce the measurement technique, present a measurement campaign, describes the novel probe-corrected near-field to far-field transform algorithm before presenting preliminary results. As this paper recounts the progress of ongoing research, it concludes with a discussion of the remaining outstanding issues and presents an overview of the planned future work.**

I. Introduction

Since its inception, the cylindrical near-field antenna measurement technique [1], [2], [3] has become a powerful method for accurately and precisely characterising the performance of medium to high gain antennas. The technique being perhaps best suited to those radiators possessing a commensurate cylindrical radiating structure corresponding to a fan-beam antenna pattern function. Whilst the conjunction of a linear translation stage and a rotation stage enables the complete far-field pattern to be determining in the azimuthal plane (assuming a vertical axis of rotation), in many practical instances the necessarily larger antenna under test (AUT) to scanning near-field probe separation, *i.e.* range length, needed to avoid mechanical interference has tended to result in these facilities being either larger, or more restricted in their capacity to determine the antenna performance in the elevation plane, than their planar counterparts.

Thus, for the case of the cylindrical near-field methodology, if the entire 4π steradian far-field pattern is to be determined exactly, either the propagating field must be sampled in the cylindrical aperture of the AUT, or over the surface of an enclosing conceptual cylinder of infinite length. In practice, due to the finite extent of the cylindrical scanning surface, any conventional cylindrical near-field measurement will inevitably represent a truncated data set, and as such, any predicted far-field pattern would include errors associated with this truncation. Furthermore, the precise nature of this effect is complicated as a variation in any part of the near-field pattern will necessarily, as a consequence of the holistic nature of the transform, result in a change to every part of the corresponding far-field pattern.

However, it is the data that is transformed to produce the far-field pattern that is required to be free from excessive truncation [4]. If this data is the product of the combination of a number of partial planar data sets that, in contrast to the partial scan data set, fulfils the transformation requirements in terms of sampling rate and continuity over the sampling interval, then the prediction will, in principle, be free from truncation errors. Indeed, exactly this strategy has been used to reduce truncation in planar near-field measurements and underpins both the auxiliary translation [5], and poly-planar [6] antenna measurement techniques. Furthermore, during the development of the poly-planar technique, it was shown through numerical simulation and experimental measurement that a flat-topped pyramid (*i.e.* a square based frustum) provided an attractive solution to the measurement of medium and high gain antenna patterns in the forward hemisphere. Here, the purpose of the flat top was to enable the intersection between adjacent scans to be chosen to be in regions of lower field intensities where imperfections in their alignment would have a less significant effect on the resulting far-field pattern. Following this reasoning, [6] proposed that a right conic frustum measurement configuration would be similarly beneficial, *c.f.* Figure 1b.

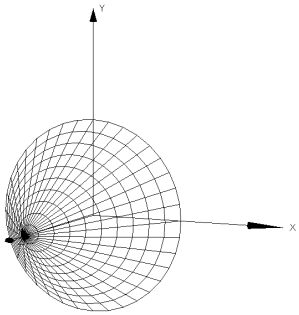

Fig. 1a Conical system

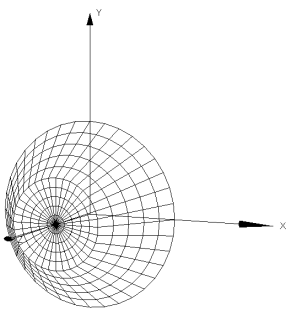

Fig 1b frustum system.

Previous workers have shown that a simple change in the alignment of a cylindrical near-field measurement system can be used to enable near-field data to be taken over the surface of a conceptual right cone, and that far-field parameters can be obtained using spherical [7], and cylindrical [8], mode expansions.

II. Overview of Measurement Technique

Conceptually, the right conical measurement system is perhaps most closely related to the well-documented, well-understood, cylindrical near-field scanning technique. Only here, the axis of rotation of the antenna under test (AUT) and the linear translation stage which caries the probe, are no longer constrained to be exactly parallel with one another. By taking samples incrementally over a raster grid by varying the azimuthal angle and linear displacement, the near electric field can be sampled over the surface of a conceptual right cone that intentionally encloses the AUT. If the near-field probe is rotated through 90° about its axis of rotation (assuming a singularly polarised probe is used, *e.g.* a rectangular open ended waveguide probe) and this process is repeated, two orthogonal near electric field components can be acquired and it is from these that the far-field pattern can be obtained. When two parallel planes truncate this right cone, a circular based right frustum is obtained. Similarly, a frustum near-field measurement is formed from the combination of two (ideally three if the back plane is also sampled) partial near-field scans. One of which consists of a conventional (typically highly truncated) plane rectilinear, or plane polar, near-field measurement, and the other a partial (*i.e.* truncated) conical near-field measurement. The frustum transformation would then take these two disparate data sets and process them to provide the equivalent far-field antenna pattern.

In order that the proposed conic-frustum near-field antenna measurement system could be verified the Queen Mary, University of London (QMUL) NSI-200V-3x3 planar near-field system was augmented with a cylindrical near-field upgraded. Thus, this combination planar/cylindrical near-field system, which is shown in Figure 2 could be used to take both planar and conical partial scans. The robotic positioner is of an inverted "T" design. This is preferable in this area of application as the scattering cross-section presented by the robotic structure is minimised. The relatively small physical dimensions of the scan plane, approximately 0.9m × 0.9m, enables both the planarity of the scanner, and the dynamic range of the RF sub-system to be maximised. As a result of this, comparatively short lengths of the RF cabling are required which is crucial at higher frequencies, or as in this case, when the AUT is not nominally aligned to the axes of the range and the measured signal is smaller. For the conical scan the position and orientation of the AUT with respect to the probe requires special consideration as it is crucial that the axis of rotation and the linear translation axis intersect and lie within the same (for convenience, vertical) plane in space. As the AUT has a compound angle it may require the fabrication of a jig to assist with any alignment of its waveguide to that of the probe via rotation of the polariser (ϕ-axis rotation stage).

Fig. 2 X-band corrugated horn shown being aligned on QMUL NSI-200V-3x3 combination planar/cylindrical system.

Alternatively, the AUT could be temporarily moved into a horizontal position by the angle plate where the AUT waveguide would be aligned to the probe via the polariser. Whichever method is used, it is important to set the polarisation to an arbitrary (but known) zero at this stage which is in alignment with the probe orientation. Care must also be given to the angle of the AUT and that of the probe. This angle should be exactly the same so the probe lies normal to the AUT axis. This requirement was introduced so that the conventional planar transmission matrix formula could be retained and when inverted, used to compensate the conical measurements without introducing any tangible practical limitations into the measurement process. It also had the benefit of helping to maximise the system RF power budget. Once the AUT is back at its correct tip angle a technique is required for locating the position of the scanner probe to the curve, *i.e.* ring, in space where the two scans intersect. An alignment jig was attached to the AUT concentric with its aperture so that it set the distance above the AUT and to its side, shown in Figure 2. Clearly, this tooling was removed during the acquisition process. In these measurements, this is referred to as "scan A" ref point. With lateral and vertical movement of the probe it is relatively easy to accurately position this to the reference point. The vertical scan parameters were then defined relative to this point. The scans where taken on the fly in the vertical linear axis and the antenna rotated in small angular steps until the full conceptual measurement cone was mapped out. Figure 3 contains a schematic representation of the measurement geometry showing that the planar measurement was taken with an AUT to probe separation of 150 mm (for the end-cap planar measurement), and the intersection of the conical and planar surfaces occurred when the planar disk had a radius of 250 mm with the half cone-angle set to 30°. The sample spacing was specified so that at least one sample was taken every half wavelength along the linear dimension, and a fixed angular increment was chosen that corresponded to one sample per half wavelength around the largest cylindrical cut. The near-

field data was acquired using a standard version of NSI2000 cylindrical near-field measurement software.

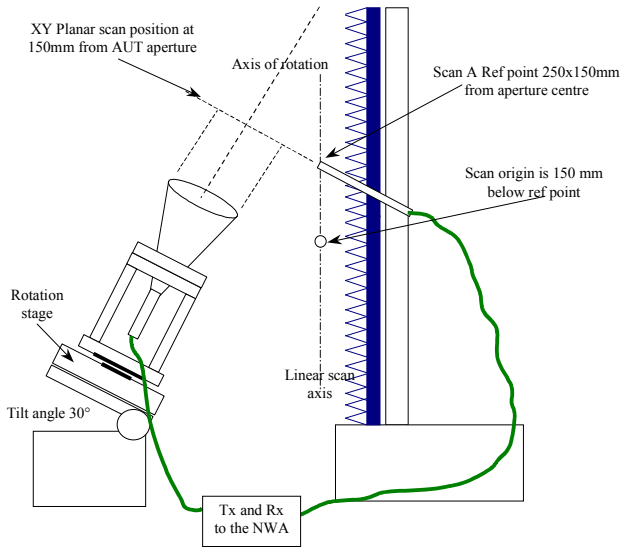

Fig. 3 Schematic of frustum measurements as taken using NSI-200V-3x3 combination planar/cylindrical system.

Here, a mechanically robust, medium gain, x-band, corrugated horn was chosen to be the AUT (which is of a class of antennas that are not generally thought to be well suited for characterisation by small planar or cylindrical scanners) so that a significant proportion of the radiated field would illuminate the sidewalls of the conceptual sampling frustum and susceptibility to gravitational deformation would not be an issue.

III. Overview of Transformation Algorithm

Conventionally when taking near-field measurements, the normal electric field component is not sampled; instead it is recovered from the tangential components via an application of the plane wave condition in the spectral domain, *i.e.* $\underline{k}\cdot\underline{E} = 0$. If the plane wave spectrum method and plane wave condition are used, and providing that the sampled data set is truncated, it is very likely that the reconstructed normal field component will be in error [4], [6]. This is obviously a problem as individually partial scans are by definition and by design truncated. Furthermore, this field component is required before the partial data sets can be combined, as the principal of superposition requires that each partial pattern be resolved onto the *same* polarisation basis. This error usually manifests itself in the form of a spurious high spatial frequency ripple that is present in the reconstructed normal electric field component. Importantly, as the magnetic field is generally obtained from the electric field and the direction of propagation, these fields would be similarly unreliable with the tangential components of the reconstructed magnetic field being most affected. Crucially, it has been found that this can be resolved by windowing the tangential electric field components before transforming to the angular spectrum. The "convoluted" normal spectral component can be obtained directly from the plane wave condition whereupon it can be inversely transformed to obtain the "windowed" normal field component. The windowing function can then be divided out to obtain reliable results providing that this function is absolutely integrable and non-zero. A detailed description of this procedure can be found in [4], and [6]. Whilst this is entirely appropriate for handling the circular disk formed by the intersection of the cone and the plane, this strategy will require modification before it is in a suitable form for use on the truncated conical section of the frustum. Indeed, the success of this windowing technique for: the recovery of the normal field component, the reconstruction of the magnetic fields, and the success of the probe pattern correction, leads to a simple question. What is the limit of how small the partial scan can be made before the filtering technique fails; and specifically, can the partial scans be collapsed to a single one-dimensional line as would be required here?

Clearly, for the windowing technique to be deployable the partial scan must be sufficiently large to enable the application of a smooth amplitude taper. However, as we are only interested in the results at a single point in space, if the near field data were to be extrapolated such that a windowing function could be usefully applied in the second dimension then, although the extrapolated results would be in error, the central point would be handled correctly. For the most elementary case, this process would consist of the following steps: extrapolate a sufficiently large data set, apply the near field window, reconstruct the normal field component, remove the window, and remove the extrapolated points so that only the normal field component corresponding to the original data points remains.

Figure 4 contains a cut that compares the normal field component having been reconstructed using a completer two-dimensional data set, and the equivalent data having been recovered using the extrapolation/windowing method on a single near field cut. Here, a cosine windowing function has been utilised but similarly encouraging results have been obtained from other windowing functions, with triangular windows also found to work well.

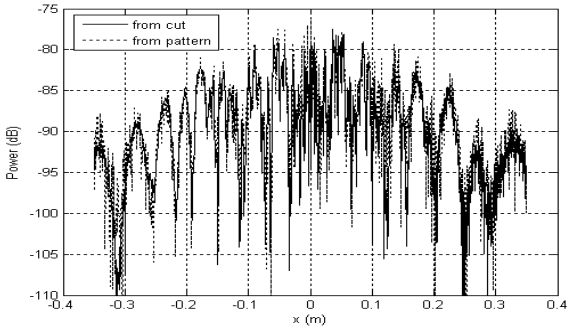

Fig. 4 Comparison of reconstructed normal field component recovered from full two-dimensional pattern and a single cut.

Since each linear cut for a given, fixed, ϕ angle can be processed using this algorithm, by stepping sequentially over all values in ϕ the complete probe pattern corrected electromagnetic six-vector can be reconstructed over the conic part of the frustum. Specifically, the sampled E_ϕ and E_z field components can be used to recover the probe compensated E_ϕ, E_z, E_ρ, H_ϕ, H_z and H_ρ field components. Here, the conversion of these electric and magnetic fields from cylindrical (recall that the near-field probe is tilted so the fields are resolved on

to a cylindrical polarisation basis, but are tabulated on a conical co-ordinate system) polarisation basis to another convenient, say Cartesian, polarisation basis is trivial. Clearly, the circular "end-cap" of the frustum measurement can be processed using the standard poly-planar partial scan field reconstruction method [4], [6]. Now that a way has been found to recover the probe corrected near-field electromagnetic six-vector, a way to obtain the corresponding asymptotic far-field pattern from this data is needed.

Generally, modal expansion techniques are inappropriate for use with bespoke (*i.e.* tailored) sampling surfaces such as those considered here as the sampling surface must correspond to a constant co-ordinate surface in the system for which the harmonic function series solutions are available. Consequently, an alternative technique that better handles discontinuities in the sampling surface than the plane wave spectrum method was sought. To this end, the Kirchhoff-Huygens (KH) formula was utilised [4] as this had been successfully harnessed within the poly-planar method. This method essentially constitutes a direct integration of Maxwell's equations with the use of a vector Green's theorem to yield an integral solution of Maxwell's equations in terms of sources, *c.f.* the Stratton-Chu solution. The choice of the field form of this method was thought to be preferable in this case as although an equivalent surface electric and surface magnetic current form of the KH formula exists and is widely used, the quantities that are sampled within the measurement are proportional to fields, not surface currents. It is applicable to arbitrary shaped apertures over which *both* the electric and magnetic fields are prescribed. The far electric field, at a point P radiated by a closed Huygens surface S is [4], [6],

$$\underline{E}_p(\hat{\underline{u}}) = \frac{\pi}{jk_0\lambda^2}\int_S \left[\hat{\underline{u}}\times(\hat{\underline{n}}\times\underline{E}) + Z_0\hat{\underline{u}}\times\{(\hat{\underline{n}}\times\underline{H})\times\hat{\underline{u}}\}\right]e^{jk_0\hat{\underline{u}}\cdot\underline{r}}da \quad (1)$$

This expression yields the asymptotic far-field vector pattern function from an integral of the electric and magnetic fields over the closed surface S (*i.e.* the frustum, which is the combination of the planar disk end-cap, and the truncated conical sides) and da is an elemental area of S and $\underline{n}$ is the outward pointing surface unit normal. Here, the r^{-1} term and the unimportant spherical phase factor have been suppressed.

IV. Preliminary Results

As described above, a modified Nearfield Systems Inc (NSI) combination planar/cylindrical near-field scanner was used to acquire two partial scans. This data was then processed using the novel probe-correcting near-field recovering algorithm and a comparison between the measured ϕ-polarised field component and the probe pattern correctedϕ-polarised field component can be seen in Figure 5a and b respectively. Here, we can see that the differences introduced into the patterns are small, as one would expect when using an electrically small probe. However, in near-field regions where the angle of incidence between the field point and the probe are larger, the effect of probe pattern correction has been to increase the field intensities, which is in broad agreement with intuition.

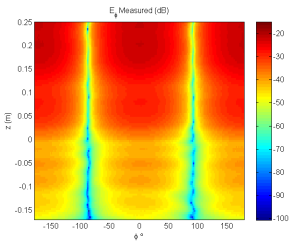

Fig. 5a E_ϕ Measured (dB)

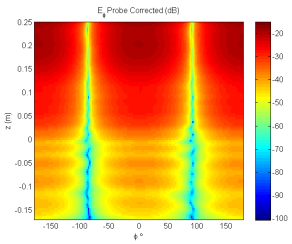

Fig. 5b E_ϕ probe-corrected (dB).

Although not shown, similar effects were observed for the orthogonally polarised tangential field component. Figure 6, contains a plot of the locally normal polarised electric field component. Although some spurious low-level high spatial frequency ripple is evident, this at a sufficiently low level that it would not be expected to pose a significant problem to the transformation process.

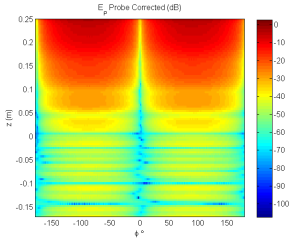

Fig. 6 Ex (dB).

Unlike cylindrical mode expansion (CME) based conical transformation techniques which require all parts of the conical sampling surface to be outside the maximum radial extent (MRE) plus two wavelengths [8], plane wave spectrum based technique presented here only require that the probe and AUT be separated by more than two wavelengths. Crucially then, this enables this PWS based techniques to be used when the radii of the cone is smaller than the MRE (*i.e.* when $z >$ 0.150 m) which provides this technique with a significant advantage. These cylindrically polarised electric and magnetic field components field components were then resolved onto a Cartesian polarisation basis ready to be transformed to the far-field. Figure 7 a, b, c, and d contains the probe corrected *x*-, *y*- and *z*-polarised electric field components plotted together with the magnitude of the near electric field respectively.

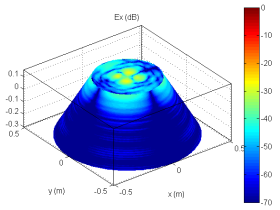

Fig. 7a E_x (dB)

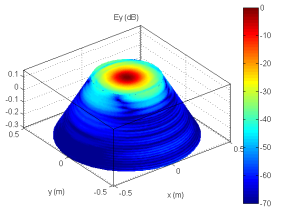

Fig. 7b E_y (dB).

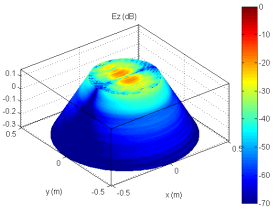

Fig. 7c E_z (dB)

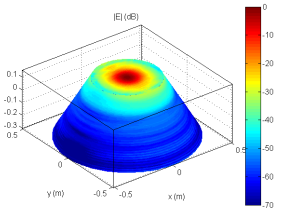

Fig. 7d |E| (dB).

Here, the two partial scans were normalised to one another by computing the magnitude of the electric field around the circular intersection between the two adjacent data sets which was required as a result of a change in the RF subsystem which occurred between successive scans. These data sets, together with the corresponding magnetic near-fields, were then transformed to the far-field using the KH method and the resulting Cartesian electric field components were then resolved onto a Ludwig III [10] copolar and cross-polar polarisation basis and can be found presented in Figure 8 tabulated on a regular azimuth over elevation co-ordinate system [6].

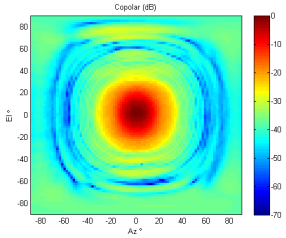

Fig. 8a copolar pattern.

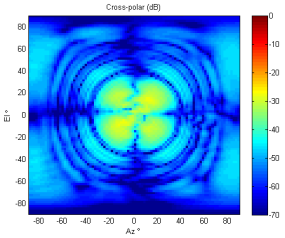

Fig 8b cross-polar pattern

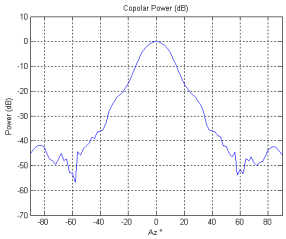

Fig. 9a Copolar azimuth cut

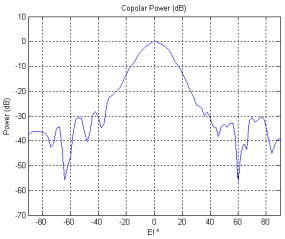

Fig. 9b Copolar elevation cut.

Figure 9a and Figure 9b contain copolar azimuth and elevation cardinal cuts respectively. Although encouraging some inaccuracies are clearly evident. Corrugated horns are renowned for their symmetry. Consequently, lack of symmetry can often be used as an indication that a measurement is unreliable. Some asymmetries are apparent but as these are only preliminary measurements requiring a great deal of development and refinement, they are none the less, encouraging results. This error can be attributed in part to recognising that the two partial scans will not intersect perfectly and that as a result of the finite measurement time and a change in the RF subsystem, some drift (both amplitude *and* phase) is contained within the measured data. Also, adverse effects of reflections from scatters within the chamber (*e.g.* the makeshift support structure, *etc*.) will inevitably degrade the far-field patterns. Another error stems from the failure to close the sampling surface. The, often, unintuitive requirement for the inclusion of the back plane follows from the requirement to perform the pattern integration required by the KH principle over a *closed* surface. Although utilising the line charge distribution method [9], which is often referred to as Kirchhoff-Kottler formulation, can ease these difficulties this technique has not yet been implemented.

V. Discussion & Conclusion

This paper has presented the use of a novel hybrid plane-wave spectrum / physical optics based probe-corrected near-field to far-field transform for use with a frustum near-field antenna measurement system. It is often preferable when taking near-field antenna measurements that a measurement geometry be selected which is commensurate with the geometry of the AUT. Thus, this technique would be particularly well suited to the characterisation of array antennas installed behind tangent ogive radomes which can constitute electrically and mechanically large test articles (which can also be unwieldy and heavy) that often present the experimenter with significant challenges.

Although only very preliminary results have been obtained and presented thus far, these are sufficiently encouraging to warrant further development effort with the future work planned to include: obtaining further measurements with particular attention being paid to accurately and precisely tying together the amplitude and phases between successive partial scans, improving the alignment between the partial scans (possible utilising optical alignment techniques), acquiring a lower gain AUT, and adjusting the measurement geometry so that a larger proportion of the radiated field illuminates the conical section which constitutes a more demanding measurement configuration (in the limit, this would result in the acquisition and transformation of a polar conical near-field measurement).

Acknowledgment

The authors wish to acknowledge AR EMV UK Ltd. for generously providing some of the test equipment that was utilised within the measurement portion of this work.

References

[1] J. Brown and E.V. Jull, "The Prediction of Aerial Radiation Patterns From Near-Field Measurements," *Proc. of the Institute of Electrical Engineers*, vol 108-B, Nov. 1961, pp. 635-644.

[2] W.M. Leach and D.T. Paris, "Probe Compensated Near-Field Measurements On A Cylinder", *IEEE Trans. on Antennas and Propagation*, AP-21, No. 4, July 1973, pp. 435-444.

[3] A.D. Yaghjian, *Near-Field Antenna Measurements "On A Cylindrical Surface: a Source Scattering-Matrix Formulation"*, Nat. Bur. Stand, NBS Tech. Note 696, July 1977.

[4] S.F. Gregson, J. McCormick, and C.G. Parini, "*Principles of Planar Near-Field Antenna Measurements*," The Institution of Engineering and Technology, IET Electromagnetic Waves series 53, December 2007, ISBN 978-0-86341-736-8.

[5] J. McCormick, and E. Da. Silva, "The Use of an Auxiliary Translation System in Near-Field Antenna Measurements", *Proc. of the Institute of Electrical Engineers 10th International Conference on Antennas and Propagation (ICAP)*, April 1997, pp. 1.90 – 1.95.

[6] S.F. Gregson, "*Probe-Corrected Poly-Planar Near Field Antenna Measurements"*, University of London Ph.D. Thesis, February, 2003.

[7] D. Leatherwood, "Conical Near-Field Antenna Measurement System", *Proc. of the Antenna Measurements and Techniques Association (AMTA) symposium*, St. Louis, November 2007.

[8] S.F. Gregson, G.E. Hindman, "Conical Near-Field Antenna Measurements," *Proc. of the AMTA symposium*, Boston, Massachusetts, November 2008.

[9] C.C. Chappas, *"The Calculation of Aperture Radiation Patterns"*, University of London Ph.D. Thesis, 1974.

[10] A.C. Ludwig, "The Definition of Cross-Polarisation", *IEEE Trans. Antennas Propagation*, vol. AP-21 no. 1, pp. 116-119, Jan. 1973.